Tuned Finite-Difference Diffusion Operators

Jason Maron[1], Mordecai-Mark Mac Low[2]

Department of Astrophysics, American Museum of Natural History, New York, NY, 10024-5192

ABSTRACT

Finite-difference simulations of fluid dynamics and magnetohydrodynamics generally require an explicit diffusion operator, either to maintain stability by attenuating grid-scale structure, or to implement physical diffusivities such as viscosity or resistivity. If the goal is stability only, the diffusion must act at the grid scale, but should affect structure at larger scales as little as possible. For physical diffusivities the diffusion scale depends on the problem, and diffusion may act at larger scales as well. Diffusivity undesirably limits the computational timestep in both cases. We construct tuned finite-difference diffusion operators that minimally limit the timestep while acting as desired near the diffusion scale. Such operators reach peak values at the diffusion scale rather than at the grid scale, but behave as standard operators at larger scales. We focus on the specific applications of hyperdiffusivity for numerical stabilization, and high Schmidt and high Prandtl number simulations where the diffusion scale greatly exceeds the grid scale.

1. Introduction

Fluid dynamics simulations usually use explicit diffusion operators, either to maintain stability or to model physical effects such as viscosity, resistivity, conductivity, or the diffusion of passive scalars. Virtually all astrophysical gas dynamics and MHD simulations rely on such diffusion operators for stability, physical effects, or both. We here consider how to design such operators such that they have the desired behavior at the diffusion scale and larger scales, while still restricting the numerical timestep as little as possible. The timestep depends inversely on the strength of the diffusion

$$\Delta t = \Delta x^2 / 2\nu. \tag{1}$$

Classical diffusion operators such as Laplacian viscosity ($\nu\nabla^2$), or fourth or sixth-order hyperdiffusivities ($\nu_4\nabla^4$ or $\nu_6\nabla^6$), reach their maximum values at the grid scale, but act at the larger diffusion scale where the effective diffusivity is lower. The operators designed here reach their maximum value at the diffusion scale rather than at the grid scale, so that they limit the timestep no more than necessary.

[1]jmaron@amnh.org

[2]mordecai@amnh.org

In a spectral code, the diffusive terms are linear and can thus be handled spectrally without limitation on the timestep. For example, let a field evolve as $\partial_t \mathbf{V} = A - \nu \boldsymbol{\nabla}^2 \mathbf{V}$, where A denotes the non-diffusive terms. In Fourier space, $\partial_t \hat{\mathbf{V}} = A - \nu k^2 \hat{\mathbf{V}}$ The solution, with A constant throughout the interval Δt, is

$$\hat{\mathbf{V}}(\Delta t) = \left[\hat{\mathbf{V}}(0) + \frac{A}{\nu k^2} (e^{\nu k^2 \Delta t} - 1) \right] e^{-\nu k^2 \Delta t} \tag{2}$$

When evolved in Fourier space, the diffusivity operator is stable for any value of $\nu k^2 \Delta t$, whereas in physical space, instability occurs if $\nu k^2 \Delta t > 2$ (restating Eq. 1 in terms of wavenumber).

However, finite difference codes do have advantages that make them worth pursuing: they use fewer floating point operations per grid point; they can be more easily parallelized without the all-to-all communications required for Fourier transforms; they are not restricted to periodic boundary conditions; and they handle discontinuous jumps more robustly.

The Navier-Stokes equation can include a number of different types of diffusion operators:

$$\begin{aligned} \partial_t \mathbf{V} &= \mathbf{V} \cdot \boldsymbol{\nabla} \mathbf{V} - \rho^{-1} \boldsymbol{\nabla} P + \nu_2 \boldsymbol{\nabla}^2 \mathbf{V} - \nu_4 \boldsymbol{\nabla}^4 \mathbf{V} + \nu_6 \boldsymbol{\nabla}^6 \mathbf{V} \\ &- \nu'_4 (\partial_x^4 + \partial_y^4 + \partial_z^4) \mathbf{V} + \nu'_6 (\partial_x^6 + \partial_y^6 + \partial_z^6) \mathbf{V} - \nu_D D[\mathbf{V}] \end{aligned} \tag{3}$$

where the ν_2 term is the usual Laplacian physical viscosity, the ν_n and ν'_n terms are nth-order hyperviscosities, the term $\nu_D D(\mathbf{V})$ is a customized diffusion operator.

Either the sixth-order hyperdiffusivity term or the physical diffusivity can maintain numerical stability. The hyperdiffusivity has been advocated (Brandenburg 2003) because it preferentially diminishes the high-wavenumber structure without modifying low-wavenumber structure. If the problem does require true physical diffusivities, we still want to consider use of a customized operator. This would reduce excess diffusion at scales well below the diffusion scale. Such excess diffusion limits the timestep without further modifying the solution as no structure exists at those scales.

To date the focus in the study of extensions to numerical diffusion has been on such hyperdiffusivities (e.g. Borue & Orszag 1995; Brandenburg 2003), as exemplified by the hyperviscosities described in equation (3). However, the degrees of freedom available in the finite difference coefficients can be used instead for different goals.

In this paper we describe methods for customizing diffusion operators that can be used to design operators that protect the timestep while either minimizing diffusion or reproducing the physical diffusion operator at low wavenumber as well as possible. These methods can also be used to design different diffusion operators for other purposes. These methods rely on the tuning techniques used by Maron et al. (2008) for improving the high-wavenumber accuracy of finite-difference derivatives.

In § 2 we summarize the constraints that lead to the need for tuning finite difference operators. We then describe operators suitable for implementing both numerical (§ 3) and physical (§ 4) diffusivities, and we summarize our results in § 5.

2. Tuning Finite Difference Operators

Let us consider the question of how to tune a general, symmetric, finite-difference operator, since all diffusion operators must be symmetric. We follow the treatment of the tuning of anti-symmetric operators such as first derivatives given in Maron et al. (2008). Such tuning allows us to customize the wavenumber spectrum of the operator to meet the needs of the problem at hand, rather than relying on simple analytic forms. This allows us, for example, in a problem with large Laplacian diffusivity, to trade small deviations from Laplacian behavior at low wavenumber for large gains in the timestep, by limiting the diffusion at high wavenumber. The deviations from Laplacian at low wavenumber can be maintained at levels small enough to not affect realistic simulations. We use both analytic solutions and numerical optimization to improve the spectral performance of the operators.

As an example of finite difference representations of symmetric operators we examine second and fourth derivatives. Define a function $f_j(x_j)$ on a set of grid points $x_j = j$, with j an integer. Then construct a finite difference operator for the second derivative $f^{[2]}$ by sampling a stencil of grid points with radius S. Without loss of generality, we center the operator on $j = 0$ and use a grid interval of $\Delta x = 1$. The familiar result for a second derivative on a radius-1 stencil is

$$\partial_x^2 f(x)|_{x=0} \sim -2f_0 + f_1 - f_{-1}, \tag{4}$$

which is obtained from fitting a polynomial of degree 2 to f_j. For a fourth derivative, we can fit a degree 4 polynomial on a radius-2 stencil,

$$\partial_x^4 f(x)|_{x=0} \sim -6f_0 + 4(f_{-1} + f_1) - (f_{-2} + f_2). \tag{5}$$

In general, a symmetric operator on a stencil of order S can be represented as

$$m_0 f_0 + \sum_{j=1}^{S} m_j (f_{-j} + f_j). \tag{6}$$

Consider the value of the finite-difference operator at $x = 0$ for a Fourier mode $f = \cos(\pi k x)$. (Sine modes can be ignored because they don't contribute to the second derivative at $x = 0$.) The wavenumber k is scaled to grid units so that $k = 1$ corresponds to the maximum (Nyquist) wavenumber $\pi(\Delta x)^{-1}$ expressible on the grid. The analytic value for the second derivative is $-\pi^2 k^2$, whereas the finite difference operator (eq. 6) gives

$$f^{[2]} \sim m_0 + 2\sum_{j=1}^{S} m_j \cos(\pi j k) \equiv -D(k) \tag{7}$$

This defines a function $D(k)$ that, when positive, acts as a diffusion applied to $f(x)$, because the Fourier modes of f evolve as $\partial_t \hat{f} = -\nu_D D(k)\hat{f}$, where ν_D is a viscosity-like parameter that sets the

level of diffusion. The maximum diffusive timestep is given by the inverse of the maximum value of $D(k)$ over $0 < k < 1$.

$$\Delta t < \frac{1}{\nu_D \max[D(k)]}. \tag{8}$$

Ideally, $D(k)$ should scale as $(\pi k)^2$ for $k < k_d$ and should be constant for $k > k_d$. The focus of this work is on customizing the form of $D(k)$ so as to to increase the maximum diffusive timestep, and, in the case of hyperdiffusion, also minimize low-k diffusion.

Figure 1 shows $D(k)$ for finite-difference stencils of radius $S = 1$ (second order) and $S = 3$ (sixth order), in comparison to the analytic value, demonstrating how higher order more closely mimics the analytic function. The coefficients of these functions are listed in Table 1. The operator $D(k)$ can be Taylor expanded in the form

$$D(k) = D_0 + D_2 k^2 + D_4 k^4 + D_6 k^6 \ldots. \tag{9}$$

An operator that reproduces ∂^2 for all k would have $D_2 = \pi^2$ and all the rest of the coefficients $D_n = 0$ for $n \neq 2$. The radius-1 stencil (Eq. 4) has $D_0 = 0$ and $D_2 = \pi^2$, but the higher order coefficients are unconstrained, while the radius-2 stencil (Eq. 4) sets $D_0 = D_4 = 0$ and $D_2 = \pi^2$.

The usual way to evaluate an operator for a function such as ∂^2 is to fit a maximal order polynomial to the points in the stencil. This yields equations that can be inverted to find the m_j coefficients in Equation 7 for stencil radius S

$$\begin{aligned} D_0 &= -m_0 - 2\sum_{q=1}^{S} m_q \\ D_p &= -\frac{2\pi^p}{p!}(-1)^{p/2} \sum_{q=1}^{S} q^p m_q, \end{aligned} \tag{10}$$

for even p. We call such operators polynomial-based operators. The form of these operators is shown in Figure 2. We may, however, use the available degrees of freedom in different ways. The goal of fitting a high-order polynomial to the derivative is to have high accuracy at high wavenumber. However, that may actually contradict the goal of protecting the timestep while either minimizing diffusion or reproducing the physical diffusion operator at low wavenumber. Instead, we can use the available degrees of freedom to directly address these requirements.

As an example, for a Kolmogorov cascade, the diffusive scale λ_ν and the viscosity ν scale as $\lambda_\nu \sim \nu^{3/4}$. The viscosity can be made sufficiently large that λ_ν is substantially larger than the grid scale, and the velocity profile will be smooth at smaller scales. The cascading energy is elminated at the diffusive scale, so there is no need for higher diffusivity at smaller scales, yet because of the form of the Laplacian diffusivity operator, the diffusivity increases all the way down to the grid scale. This excess diffusivity is unnecessary, and in fact is a liability because it restricts the timestep.

Laplacian diffusion operators, or steeper operators such as hyperdiffusivities, rise in amplitude monotonically all the way to the Nyquist wavenumber $k = 1$. A large value of $D(1)$ requires a small timestep, but is unnecessary because energy cascading from higher scales is removed earlier at the diffusion scale k_d. $D(k)$ need only have enough presence above k_d to diffuse any Fourier modes that might arise there. For $k > k_d$, it can be as large as it is at k_d with no additional timestep penalty.

This allows us to specify a strategically chosen diffusion operator that satisfies these requirements. Such an operator should rise through the diffusion range k_d, but then flatten out and merely remain positive at $k > k_d$. Since this constraint is much less critical than having controlled diffusion at low k, the low-k range of $D(k)$ should receive a higher priority in the optimization than the high-k range.

The behavior of the diffusion function at k_d critically determines its effect on the solution. The diffusion must act above both the Nyquist scale $k_{NY} = 1$, for stability, and at the resolution scale, to damp modes with wavenumbers too large to be accurately captured by the finite difference scheme. The resolution scale depends on the details of the method. However, the common choice of radius-3 stencils have a resolution scale $k = 1/2$ (Maron et al. 2008), so we choose in this work to use a diffusion scale $k_d = 1/2$, and examine diffusion functions normalized to $D(k_d) = 1$.

We note in passing that if the diffusivity is weak enough to not limit the timestep, it does not have to be applied every timestep. The diffusivity can instead be applied once every N timesteps with a value of of ν that is N times as large, for reasonable values of N (Maron et al. 2008). However, the enhanced diffusivity may then be large enough that the flat diffusivities described in this paper are required to protect the timestep. This yields a computational savings from not having to calculate the diffusion operator every timestep.

In the next two sections we describe how we perform the tuning and give some useful examples of operators for both hyperdiffusivity and Laplacian diffusivity.

3. Timestep-friendly hyperdiffusion

In situations where one wishes to maximize the scale range, and where the diffusion-scale dynamics don't affect larger scales, one can fruitfully use a diffusion operator that rises more rapidly with k than a Laplacian. Writing the diffusive terms from equation 3 in Fourier space,

$$\partial_t \hat{\mathbf{V}} = -\nu_2 k^2 \hat{\mathbf{V}} - \nu_4 k^4 \hat{\mathbf{V}} - \nu_6 k^6 \hat{\mathbf{V}} - \nu_4' (k_x^4 + k_y^4 + k_z^4) \hat{\mathbf{V}} - \nu_6' (k_x^6 + k_y^6 + k_z^6) \hat{\mathbf{V}} - \nu_d D(k) \hat{\mathbf{V}} \quad (11)$$

one sees that hyperdiffusive terms such as those proportional to ν_4 and ν_6 have a steeper dependence on the wavenumber k than the Laplacian diffusivity proportional to ν_2.

However, energy cascading from larger scales dissipates at the diffusion scale $k_d < 1$, so increasing the diffusion at $k > k_d$ further is unnecessary. A customized diffusion operator $D(k)$ can be constrained to have a similarly steep k dependence at low k, but to then flatten at the diffusion

scale k_d, so that the value at the Nyquist wavenumber $D(1)$ is not markedly higher. Since the timestep is limited by the maximum diffusivity on the grid at any scale, limiting the value of D at small wavenumber protects the timestep.

We note in passing that the ν_4 term in Equation (11) contains two successive Laplacians and therefore two rounds of finite differences, whereas terms such as $(\partial_x^4 + \partial_y^4 + \partial_z^4)$ and $D(k)$ involve only one round of finite differences, and are therefore favored for their execution speed. Also, the diffusion function for $\boldsymbol{\nabla}^4$ has a greater value in the high-k "corners" of Fourier space than $(\partial_x^4 + \partial_y^4 + \partial_z^4)$, and hence a smaller maximum diffusive timestep, and so for this reason as well, operators such as $\boldsymbol{\nabla}^4$ and $\boldsymbol{\nabla}^6$ are disfavored.

We begin by considering diffusion operators with a stencil radius $S = 3$, such as are used in the hyperdiffusion implemented in the Pencil code (Brandenburg & Dobler 2002). In this case, one can analytically construct a one-parameter family of functions parameterized by the degree of diffusivity $D(1)$ at $k = 1$. As before, we take $D(0) = 0$, the diffusion scale $k_d = 1/2$, and normalize $D(k)$ so that $D(1/2) = 1$. Inverting Equation 7 with these conditions yields

$$m_0 = -\frac{1}{2} - \frac{1}{4}D(1) \tag{12}$$

$$m_1 = \frac{1}{8} + \frac{7}{32}D(1) \tag{13}$$

$$m_2 = \frac{1}{4} - \frac{1}{8}D(1) \tag{14}$$

$$m_3 = -\frac{1}{8} + \frac{1}{32}D(1) \tag{15}$$

$$\tag{16}$$

This also implies that

$$D_4 = \pi^4 \left(\frac{1}{8} - \frac{D(1)}{16} \right). \tag{17}$$

The magnitude of D_4 is inversely related to the sharpness of the hyperdiffusive filter. Sharpness of hyperdiffusivity is usually measured by giving the index of the scaling with wavenumber k at low k. In this example, however, all the functions we present have k^4 scaling at low k and are normalized at k_d, so the lower the value of the coefficient D_4 of the k^4 term, the sharper the hyperdiffusivity.

The free parameter $D(1)$ traces the maximum diffusivity, at least in the regime $D(1) > 2$, as shown in Figure 3, and thus determines the timestep. This can be demonstrated by differentiating $D(k)$ (Eqs. 7 and 2) and showing that in this regime, $D'(k) > 0$, so $D(k)$ monotonically increases between $0 < k < 1$. For $1 < D(1) < 2$, the maximum diffusivity is not much greater than the diffusivity at $k = 1$. For example, for $D(1) = 1.5$, the maximum diffusivity is $D = 1.63$ at $k = 0.762$. The useful range for $D(1)$ is $1 < D(1) < 8$ because the case $D(1) = 8$ corresponds to the operator for ∂^6, which represents the $S = 3$ hyperdiffusivity operator that is least diffusive at low wavenumber. Choosing $D(1) > 8$ results in $D(k) < 0$ for some value of $k < k_d$. The choice $D(1) = 8$ corresponds to the standard hyperdiffusivity used in the Pencil code. We further find that the best choice to

minimize diffusivity at low k is given by requiring that $D''(0) = 0$. If $D''(0) < 0$, then $D(k) < 0$ at low k, and hence unstable, while for $D''(0) > 0$, it is more diffusive at low k than it could be.

The goals of minimizing the low-k diffusivity and protecting the timestep at high k are at odds if one normalizes the diffusion magnitude at the diffusion scale $D(k_d) = 1$. The tradeoffs can be seen by considering the behavior of $D(k)$ as $D(1)$ is increased (Fig. 3). Reducing the diffusion for $k < k_d$ requires increasing the diffusion for $k > k_d$, and vice versa. Although the values are much larger at high wavenumber, the percentage changes are actually similar in the two regimes (see Tab. 2 for the low wavenumber values).

Note that the function with $D(1) = 4$ is the standard hyperdiffusion with stencil radius $S = 2$, which is the most hyperdiffusive $S = 2$ operator. Adding one extra free parameter by moving to stencil size $S = 3$ allows both low and high wavenumber diffusivity to be tuned, but we cannot decrease both simultaneously. However, adding another free parameter by using stencil size $S = 4$ does allow both to be decreased (Fig. 2). As an additional example, note that the dotted line in Fig. 3 shows the $S = 1$ diffusivity, while the $S = 3$ result with $D(1) = 1.5$ has decreased diffusivity for both low and high k. Simultaneously decreasing the diffusion for $k < k_d$ and $k > k_d$ while maintaining a constant diffusion at $k = k_d$ thus clearly requires more than one free parameter. With two or more free parameters, we can simultaneously satisfy both goals.

Extending the stencil size to $S > 3$ allows us to further optimize the diffusion function. We now have multiple ways in which we could proceed. We choose to use numerical optimization to derive tuned $S > 3$ operators based on the following conditions: normalize the diffusion spectrum to $D(k_d) = 1$; insist that $0 < D(k) < \delta$ for some chosen value of the constant δ; set $D(0) = 0$; and require that D monotonically increase for $k < k_d$. Within these constraints, we maximize $D'(k_d)$, which measures the sharpness of the operator at k_d.

To find the operator satisfying these conditions we use a multiparameter optimization of the coefficients m_j in order to maximize $D'(k_d)$ within the constraints. We have developed a novel Monte Carlo routine to perform the optimization. It evolves the solution by testing randomly selected nearby points, selecting the best among them and iterating with a search radius sensitive to the speed of improvement of the solution. Because different parameters have widely varying ranges, we use a logarithmic sampling distribution.

In Figure 2 we show the resulting optimized diffusivities for $S = 4$ and $S = 5$. The coefficients for these operators are given in Table 3. Comparing the $S = 2$ hyperdiffusivity to the optimized $S = 4$ operator gives another example of the benefit of taking advantage of two free parameters.

4. Timestep-friendly Laplacian diffusion

Some applications require such large physical diffusivity that it becomes the dominant constraint on the timestep. Examples include magnetized turbulent flows with separated viscous and

Table 1: Coefficients for timestep-friendly Laplacian diffusion operators

	m_0	m_1	m_2	m_3	m_4	m_5
∂^2, 2^{nd} order	-2	1	···	···	···	
∂^2, 6^{th} order	-2.72222	1.5	-0.15	0.01111	···	···
k_d=1/2	-1.514721	0.5692471	0.2524535	-0.0643401	···	···
k_d=3/8	-0.9148711	0.2609054	0.2059354	-0.0094052	···	···
k_d=1/4	-0.4334820	0.0752718	0.0696988	0.0717703	···	···
k_d=7/32	-0.2733333	0.0179722	0.0172444	0.1014500	···	···
k_d=3/16	-0.2679784	0.0393498	0.0283651	0.0304570	0.0358173	···
k_d=9/64	-0.1317918	0.0097316	0.0094934	0.0088189	0.0081529	0.0296992
k_d=3/32	-0.0585600	0.0029213	0.0030688	0.0029842	0.0027554	0.0026748

Note. — The coefficients for a finite difference operator for ∂_x^2. The 2nd and 6th order entries are for a polynomial fit on a radius 1 and 3 stencil, respectively. The "k_d" entries are the tuned diffusion operators discussed in § 4.These functions are shown in Figure 1. The last entry, for $k_d = 3/32$, additionally has $m_6 = 0.0024189$, $m_7 = 0.0024876$ and $m_8 = 0.0099690$.

Table 2: Radius-3 tuned diffusion values

$D(1/4)$	$D(1/3)$	$D(1)$
.124	.328	1.5
.116	.312	2.0
.101	.281	3.0
.086	.250	4.0
.055	.187	6.0
.025	.124	8.0

Note. — Values of the diffusion function $D(k)$ for $k = 1/4$, $k = 1/3$, and $k = 1$, for the sequence of radius-3 timestep-friendly hyperdiffusion functions with varying values of $D(1)$.

Table 3: Coefficients for timestep-friendly hyperdiffusion operators

	m_0	m_1	m_2	m_3	m_4	m_5
∂^4, 4th order	1.500000	-1.	0.250000	···	···	···
∂^4, 6th order	1.750000	-1.218750	0.375000	-0.031250	···	···
Tuned, stencil 4	1.231682	-0.775549	0.074534	0.126481	-0.041307	···
Tuned, stencil 5	0.911455	-0.511864	-0.033699	0.094005	0.010574	-0.014743

resistive scales so that the magnetic Prandtl number

$$P_m = \frac{\nu}{\eta} \tag{18}$$

is far from unity, where η is the resistivity; and turbulence with a passive scalar such as temperature that diffuses at a scale different from the viscous scale so that the Schmidt number

$$S = \frac{\nu}{\kappa} \tag{19}$$

is far from unity, where κ is the diffusivity of the passive scalar. In this case, the physical diffusivity operators can also be adjusted so as to cause less harm to the timestep.

The procedure that we used to generate coefficients for flat Lagrangian diffusion operators is to specify a value for k_d, and then constrain D so as to not further increase beyond its value at the diffusion scale. Specifically, we set $D(k) < (\pi k_d)^2$ for all k. Within this constraint, we minimize the value of $(\pi k_d)^2 - D(k)$ over $k > k_d$. For a radius $S = 3$ stencil, this procedure works for k_d as low as 7/32. Any lower than that and $D(k) < (\pi k_d)^2$ cannot be satisfied without $D(k)$ taking on a dangerously small value for some $k > k_d$, or even worse, becoming negative. However, increasing the stencil size beyond $S = 3$ allows for flat diffusion operators with successively lower values of k_d. Such operators are shown in Table 1, and Figure 1 for $S = 3$.

5. Summary

We have presented techniques for customizing diffusion filters with the goal of either decreasing low-k diffusion, or maximizing the timestep, or some combination of both. We have given concrete examples that cover the commonly encountered cases, but since the requirements for diffusion can be problem dependent, we also emphasize techniques for customizing general diffusion filters.

Turbulent flows offer a major example of the need for careful choice of the magnitude of either physical diffusivity or hyperdiffusivity. The relevant magnitude is that at the diffusion scale $\nu D(k_d)$, where k_d is chosen to match the spectral resolution of the numerical scheme (Maron et al. 2008). There it must be large enough to absorb the energy from the turbulent cascade reaching that scale. The value of ν is generally set empirically to satisfy this requirement.

The techniques developed here can also be applied to models with Prandtl and Schmidt numbers that are large or small compared to unity, as well as models with diffusive chemistry.

We thank J. S. Oishi for useful discussions. We acknowledge partial support of this work by NSF grant AST06-12724, and NASA grant NNX07AI74G.

REFERENCES

Brandenburg, A. 2003, in Advances in nonlinear dynamos, eds. A. Ferriz-Mas & M. Núñez, (Taylor & Francis, London), 269

Brandenburg, A. & Dobler, W. 2002, Comput. Phys. Commun. 147, 471-475

Borue, V., & Orszag, S. A. 1995, Phys. Rev. E, 51, R856

Canuto, C., Hussaini, M. Y., Quarteroni, A., Zhang, t. A. 1987, "Spectral Methods in Fluid Dynamics," Springer-Verlag

Dedner, A., Kemm, F., Kroner, D., Munz, C.-D., Schnitzer, T. & Wesenberg, M. 2002, JCP 175, 645

Dunigan, T. 2004, www.csm.ornl.gov/ dunigan

Frigo, M., & Johnson, S. G. 1998, ICASSP conference proceedings, vol. 3, pp. 1381-1384, "FFTW: An Adaptive Software Architecture for the FFT."

Lele, S. K. 1992, J. Comp. Phys. 103, 16

Londrillo, P. & Del Zanna, L. 2000, ApJ 530, 508

Maron, J., Mac Low, M.-M., & Oishi, J. S. 2008, ApJ, 677, 520

Maron, J. & Goldreich, P. 2001, ApJ, 554, 1175

San Diego Supercomputing Center technical specifications, 2003, `www.sdsc.edu/PMaC/Benchmark/maps_ping/maps_ping_results.html`

Stone, J. & Norman, M. 1992a, ApJS, 80, 753

Stone, J. & Norman, M. 1992b, ApJS, 80, 791

Tamm, C. & Webb, J. 1993, JCP 197, 262

Toth, G. 2000, JCP, 161, 605

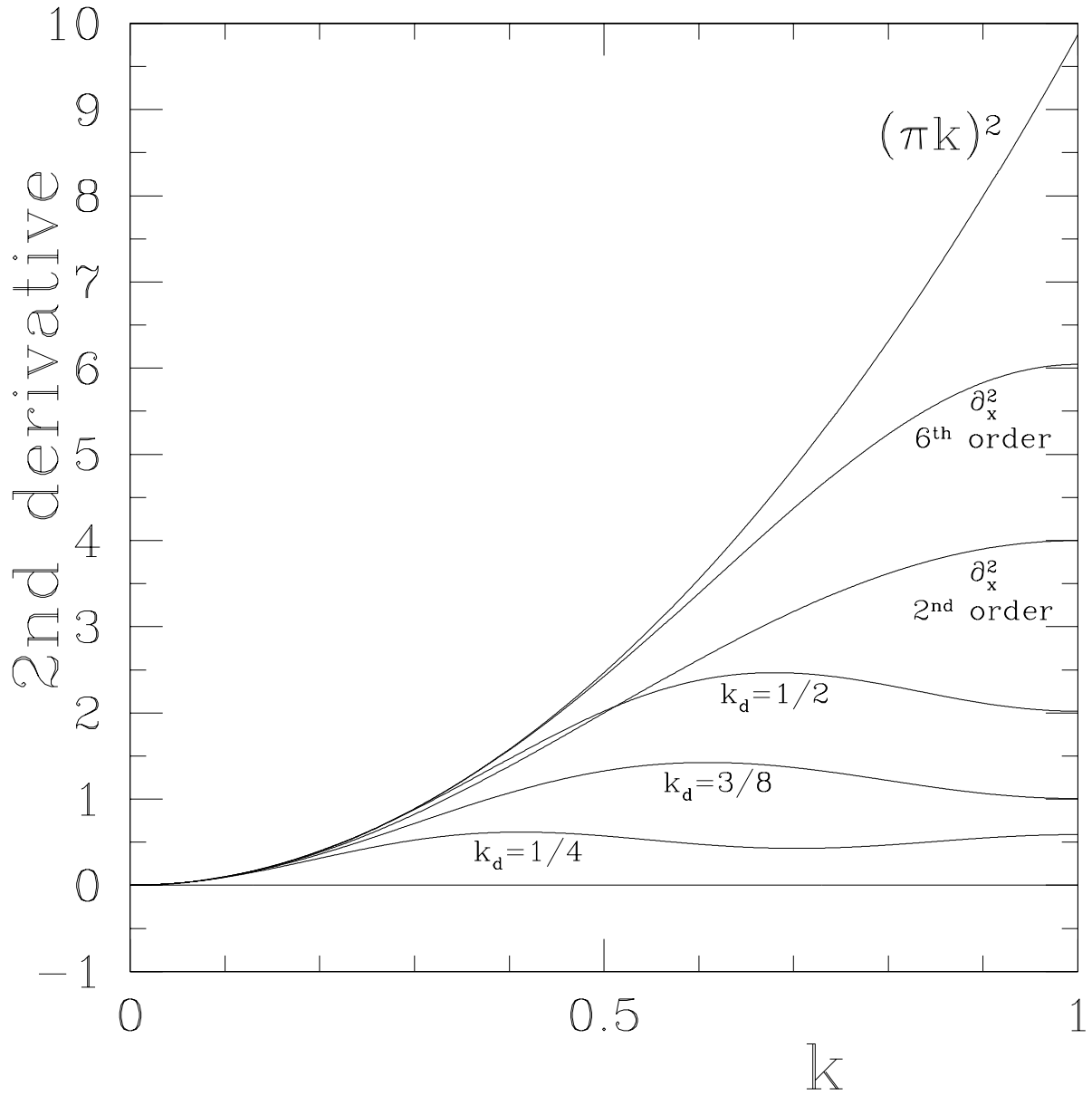

Fig. 1.— Values of $\partial_x^2 \cos(\pi k x) = (\pi k)^2$, and the different finite difference operators having coefficients listed in Table 1. Two examples of polynomial-based difference operators with stencil radii $S = 1$ and highest order two and $S = 3$ and highest order six are shown, along with three examples of operators tuned with different choices of the beginning of the diffusive range k_d.

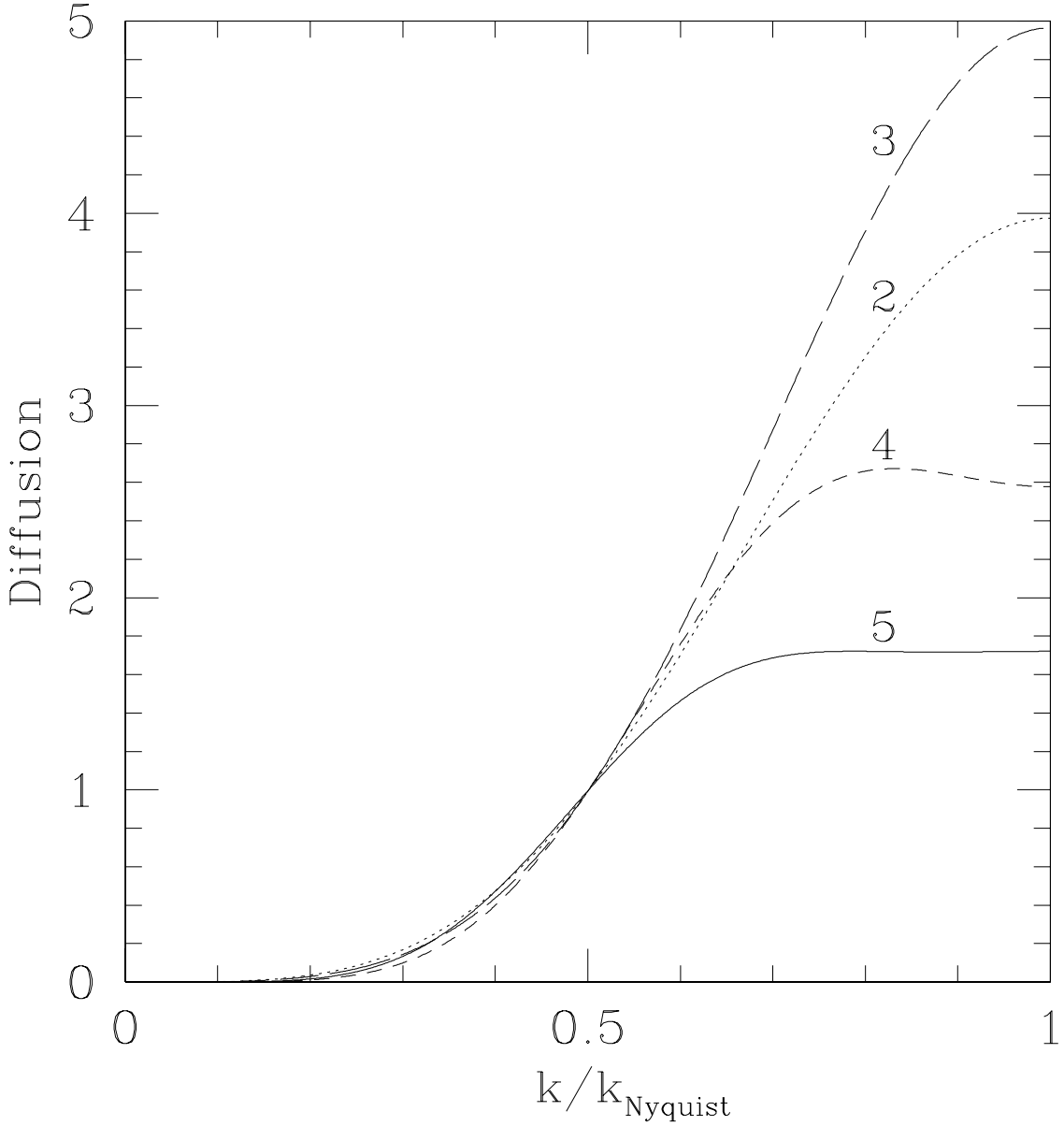

Fig. 2.— Timestep-protecting diffusion functions are compared to standard hyperdiffusivities. Each of these functions approaches $k = 0$ approximately as k^4, and each has been normalized so that $D(1/2) = 1$. The function labeled "2" is the radius-2 stencil finite-difference formula for ∂^4, or in other words, a $\boldsymbol{\nabla}^4$ hyperdiffusivity. The function labeled "3" is the radius-3 stencil finite-difference formula for ∂^4. Since it is higher-order, it more faithfully represents the function k^4 for large k. However, this is a liability for the timestep because it is more vulnerable to a diffusive timestep instability at $k = 1$ than the radius-2 function. The function labeled "4" has a different objective. It is a radius-4 stencil finite-difference formula for ∂^4, but instead of using the extra degrees of freedom to represent k^4 at higher order, they are used to minimize $D(k)$ for $k > 1/2$. The function labeled "5" has the same goal as "4" implemented with a radius-5 stencil.

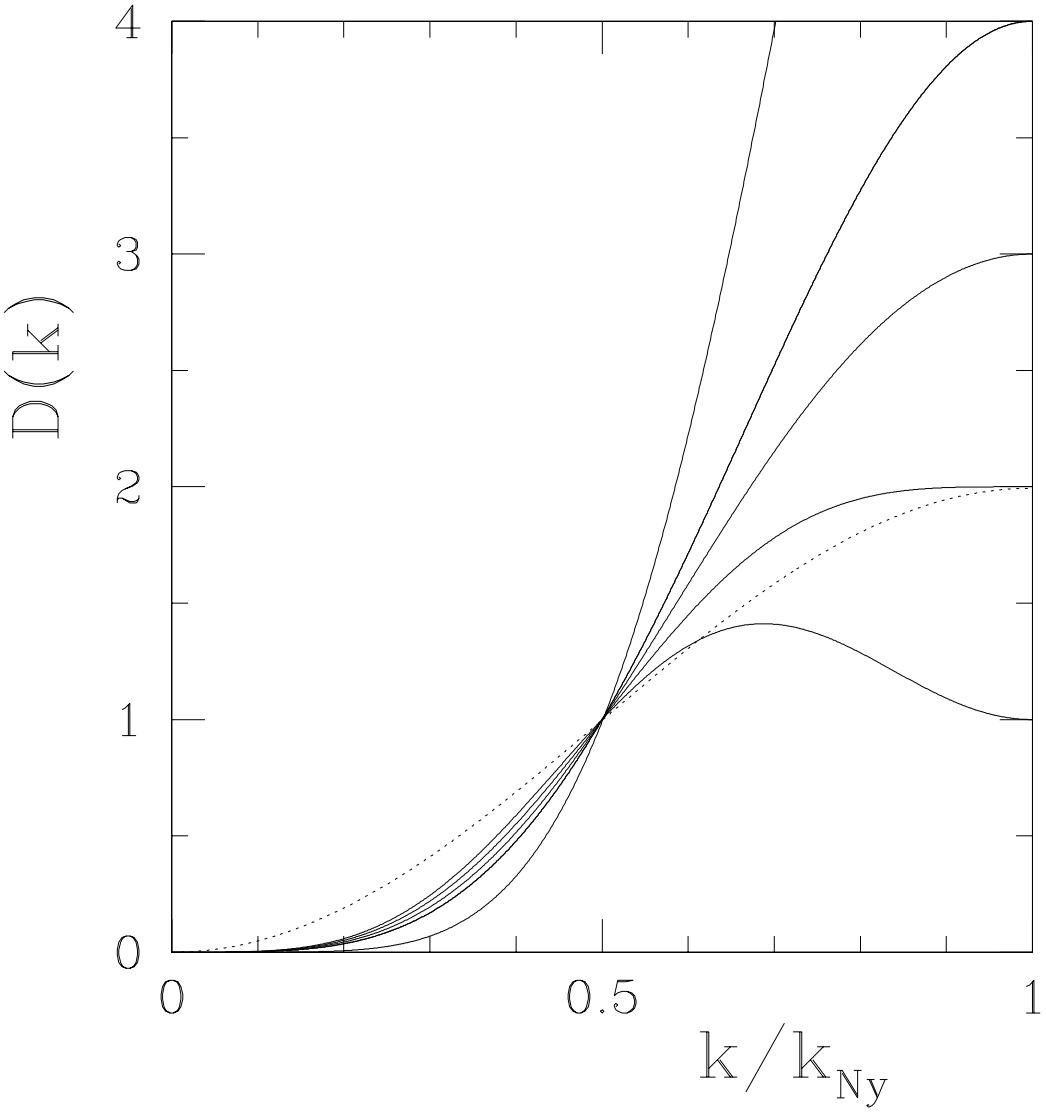

Fig. 3.— The family of diffusion functions $D(k)$ for $1 < D(1) < 8$ for a stencil with radius $S = 3$, represented with solid lines. The dotted line shows the $S = 1$ operator for ∂^2; the addition of the two additional parameters in the $S = 3$ operator allowed reduction of diffusivity at both high and low wavenumber while maintaining the normalization at k_d. The $D(1) = 4$ line is identical to the standard $S = 2$ hyperdiffusivity. The functions are all continuous through $D(k_d)$, so the most diffusive above k_d are the least diffusive below it.